

Solution Calorimetric Investigation of Oxidative Addition of HEAr (E = O, S, Se; Ar = C₆H₄X, X = CH₃, H, Cl, NO₂) to (PMe₃)₄Ru(C₂H₄): Relationship between HEAr Acidity and Enthalpy of Reaction[†]

Jinkun Huang, Chunbang Li, and Steven P. Nolan^{*,‡}

Department of Chemistry, University of New Orleans, New Orleans, Louisiana 70148

Jeffrey L. Petersen

Department of Chemistry, West Virginia University, Morgantown, West Virginia 26506-6045

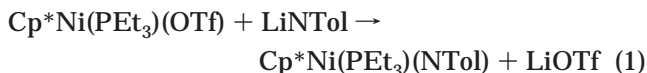
Received April 2, 1998

The enthalpies of reactions of (PMe₃)₄Ru(C₂H₄) (**1**) with a series of HEAr compounds (E = O, S, Se; Ar = aryl), leading to the formation of (PMe₃)₄Ru(H)(EAr) complexes, have been measured by anaerobic solution calorimetry in C₆H₆ at 30.0 °C. These reactions are rapid and quantitative under the calorimetry conditions. The measured reaction enthalpies span a range of some 35 kcal/mol. The relative stability scale established is as follows: (PMe₃)₄Ru(H)(OC₆H₄-*p*-CH₃) < (PMe₃)₄Ru(H)(OC₆H₅) < (PMe₃)₄Ru(H)(OC₆H₄-*p*-Cl) < (PMe₃)₄Ru(H)(OC₆H₄-*p*-NO₂) < (PMe₃)₄Ru(H)(SC₆H₄-*p*-CH₃) < (PMe₃)₄Ru(H)(SC₆H₅) < (PMe₃)₄Ru(H)(SC₆H₄-*p*-Cl) ≈ (PMe₃)₄Ru(H)(SeC₆H₅) < (PMe₃)₄Ru(H)(SC₆H₄-*p*-NO₂). A single-crystal X-ray structure of one of these complexes, (PMe₃)₄Ru(SC₆H₅)H (**7**), is reported. The measured enthalpies of reaction display a dependence on the acidity of HEAr.

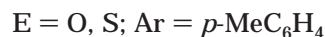
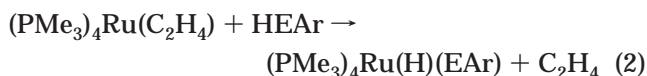
Introduction

Oxidative addition and reductive elimination reactions are critical processes in the catalytic and stoichiometric applications of transition-metal reagents in organic synthesis.¹ The oxidative addition of C–H bonds across a metal center has been the focus of much attention in view of the interest in alkane activation and functionalization.² Much less is known of the activation of E–H bonds, where E is a heteroatom (O, S, Se, N, P). Transition-metal complexes bearing anionic oxygen and nitrogen ligands represent important intermediates in industrial^{3,4} and biological processes.⁵ Recent developments in this area have lead to the formation of novel metal alkoxides,⁶ arylamides,⁷ thiolates,⁸ and phosphides.⁹ The major synthetic route employed to form these complexes has been the metathesis of a metal

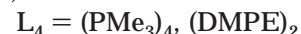
halide (or equivalent) and an alkali metal salt of the heteroatom-containing anion. A recent example of this metathesis route is shown in eq 1.¹⁰



An alternative strategy has been presented by Bergman and co-workers in which oxidative addition of HX to a Ru(0) center yields a series of interesting Ru(II) complexes (eq 2 and 3).¹¹ Although these systems have



X = NHPH, PHPh, OAr, SAR;



been fully characterized and the thermodynamic driving forces behind important ligand-exchange processes have been qualitatively addressed, no quantitative thermodynamic information is available on these processes.

(10) Holland, P. L.; Andersen, R. A.; Bergman, R. G.; Huang, J.; Nolan, S. P. *J. Am. Chem. Soc.* **1997**, *119*, 12800–12814.

(11) (a) Burn, M. J.; Fickes, M. G.; Hollander, F. J.; Bergman, R. G. *Organometallics* **1995**, *14*, 137–150. (b) Hartwig, J. F.; Andersen, R. A.; Bergman, R. G. *Organometallics* **1991**, *10*, 1875–1887.

[†] This contribution is dedicated to Professor Carl Hoff, friend and mentor, on the occasion of his 50th birthday.

[‡] E-mail: spncm@uno.edu.

(1) Collman, J. P.; Hegedus, L. S.; Norton, J. R.; Finke, R. G. *Principles and Applications of Organotransition Metal Chemistry*; University Science Books: Mill Valley, CA, 1987.

(2) Arndtsen, B. A.; Bergman, R. G. *Science* **1995**, *270*, 1970–1973 and references cited.

(3) Roundhill, D. M. *Chem. Rev.* **1992**, *92*, 1–27.

(4) Bryndza, H. E.; Tam, W. *Chem. Rev.* **1988**, *88*, 1163–1188.

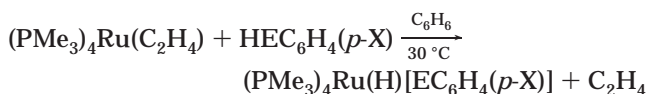
(5) Holm, R. H.; Kennepohl, P.; Solomon, E. I. *Chem. Rev.* **1996**, *96*, 2239–2314 and other articles in this issue.

(6) Glueck, D. S.; Winslow, L. N.; Bergman, R. G. *Organometallics* **1991**, *10*, 1462–1479.

(7) (a) Driver, M. S.; Hartwig, J. F. *J. Am. Chem. Soc.* **1996**, *118*, 7217–7218. (b) Mann, G.; Hartwig, J. F. *J. Am. Chem. Soc.* **1996**, *118*, 13109–13110. (c) Woffe, J. P.; Wagaw, S.; Buckwald, S. L. *J. Am. Chem. Soc.* **1996**, *118*, 7215–7216.

(8) Milstein, D.; Calabrese, J. C.; Williams, I. D. *J. Am. Chem. Soc.* **1986**, *108*, 6387–6389.

(9) Bohle, D. S.; Jones, T. C.; Rickard, C. E. F.; Roper, W. R. *J. Chem. Soc., Chem. Commun.* **1984**, 865–867.

Table 1. Solution Enthalpies of Reaction (kcal/mol) for

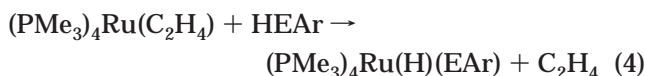
complex	E	X	$-\Delta H_{\text{rxn}}^a$
2	O	CH_3	4.1(2)
3	O	H	6.1(2)
4	O	Cl	7.0(3)
5	O	NO_2	13.2(2)
6	S	CH_3	28.3(4)
7	S	H	30.6(3)
8	S	Cl	32.0(2)
9	S	NO_2	39.0(2)
10	Se	H	32.5(3)

^a Enthalpy values are reported with 95% confidence limits.

Elaborating on our earlier ruthenium thermochemical studies,¹² we present in this paper a solution calorimetric investigation of the oxidative addition to an electron-rich ruthenium(0) center.

Results and Discussion

Thermochemistry. A solution calorimetric investigation of the oxidative addition of a number of weak proton-donor electrophiles is made possible by the rapid displacement of ethylene from $(\text{PMe}_3)_4\text{Ru}(\text{C}_2\text{H}_4)$ (**1**), eq 4. The electronic properties of HEAr can be modulated



by varying E as well as the substituents on the Ar group. To quantify the enthalpic effects associated with these electronic variations, anaerobic solution calorimetry measurements involving **1** and a series of HEAr compounds were performed in benzene at 30 °C. All reactions investigated proved rapid and quantitative under calorimetric conditions. The utilization of **1** as a thermochemical anchor point permits the construction of a relative stability scale which includes 10 ruthenium complexes. Enthalpy data are presented in Table 1.

Thermochemical Effects of Electronic Variations within the $\text{HEC}_6\text{H}_4\text{X}$ Series ($\text{E} = \text{O}$, $\text{X} = \text{CH}_3$ (2**), H (**3**), Cl (**4**), NO_2 (**5**); $\text{E} = \text{S}$, $\text{X} = \text{CH}_3$ (**6**), H (**7**), Cl (**8**), NO_2 (**9**)).** A number of variations are brought about in this series by affecting the electronic donation

(12) (a) Nolan, S. P.; Martin, K. L.; Stevens, E. D.; Fagan, P. J. *Organometallics* **1992**, *11*, 3947–3953. (b) Luo, L.; Fagan, P. L.; Nolan, S. P. *Organometallics* **1993**, *12*, 4305–4311. (c) Luo, L.; Zhu, N.; Zhu, N.-J.; Stevens, E. D.; Nolan, S. P.; Fagan, P. J. *Organometallics* **1994**, *13*, 669–675. (d) Li, C.; Cucullu, M. E.; McIntyre, R. A.; Stevens, E. D.; Nolan, S. P. *Organometallics* **1994**, *13*, 3621–3627. (e) Luo, L.; Nolan, S. P. *Organometallics* **1994**, *13*, 4781–4786. (f) Cucullu, M. E.; Luo, L.; Nolan, S. P.; Fagan, P. J.; Jones, N. L.; Calabrese, J. C. *Organometallics* **1995**, *14*, 289–296. (g) Luo, L.; Li, C.; Cucullu, M. E.; Nolan, S. P. *Organometallics* **1995**, *14*, 1333–1338. (h) Serron, S. A.; Nolan, S. P. *Organometallics* **1995**, *14*, 4611–4616. (i) Serron, S. A.; Luo, L.; Li, C.; Cucullu, M. E.; Nolan, S. P. *Organometallics* **1995**, *14*, 5290–5297. (j) Li, C.; Ogasawa, M.; Nolan, S. P.; Caulton, K. G. *Organometallics* **1996**, *15*, 4900–4903. (k) Serron, S. A.; Luo, L.; Stevens, E. D.; Nolan, S. P.; Jones, N. L.; Fagan, P. J. *Organometallics* **1996**, *15*, 5209–5215. (l) Li, C.; Olivan, M.; Nolan, S. P.; Caulton, K. G. *Organometallics* **1997**, *16*, 4223–4225. (m) Serron, S. A.; Nolan, S. P.; Abramov, Y. A.; Brammer, L.; Petersen, J. L. *Organometallics* **1998**, *17*, 104–110.

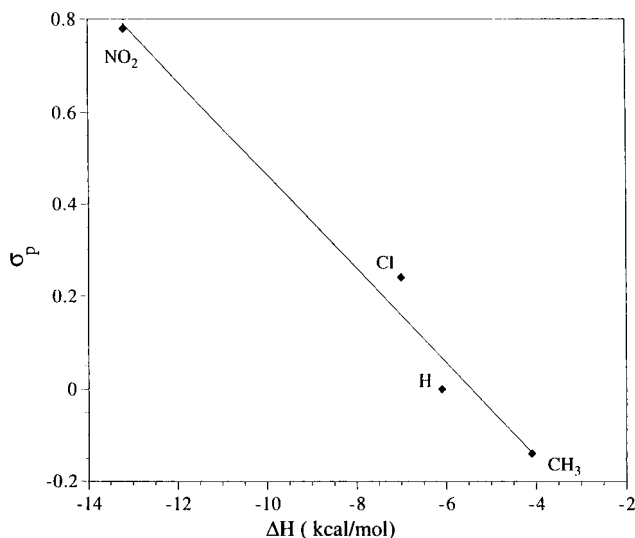


Figure 1. Hammett σ_p parameter versus enthalpies of reaction (kcal/mol) for the $(\text{PMe}_3)_4\text{Ru}(\text{H})(\text{OC}_6\text{H}_4\text{X})$ system; slope = -0.10 , $R = 0.99$.

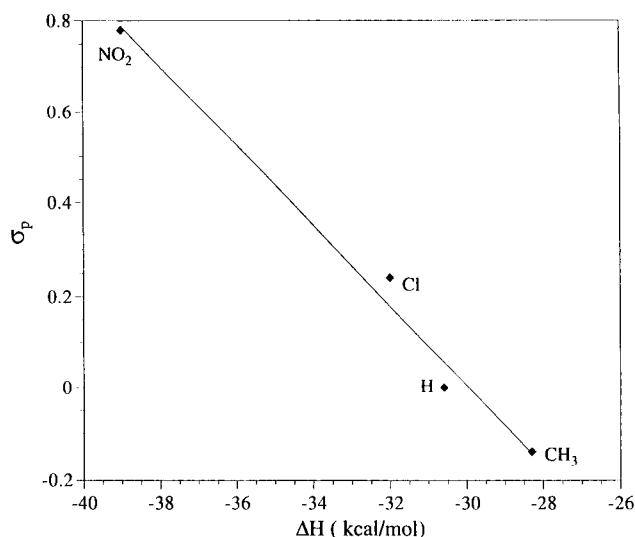


Figure 2. Hammett σ_p parameter versus enthalpies of reaction (kcal/mol) for the $(\text{PMe}_3)_4\text{Ru}(\text{H})(\text{SC}_6\text{H}_4\text{X})$ system; slope = -0.09 , $R = 0.99$.

of the aryl moiety by selecting substrates with varying substituent electronic properties in the trans position to the heteroatom. This effect spans a range of 9 kcal/mol for the phenols and 11 kcal/mol within the thiophenol series. This para-substituent effect can be thought of in terms of the Hammett parameter σ_p .¹³ A simple thermochemical relationship can be established between the enthalpies of reaction and the Hammett parameter characterizing the inductive effect at play. Such relationships for the phenols and thiophenols are presented in Figures 1 and 2. Both relationships display similar slopes and span a similar range, indicating that similar influences are felt at the metal binding site.

A second property of the acidic reactants which is influenced by the inductive effects of the para-substituent is their $\text{p}K_a$.¹⁴ In view of this relationship and since the Hammett σ_p parameter and $\text{p}K_a$ correlate linearly,

(13) Hammett σ_p values are taken from Isaacs, N. *Physical Organic Chemistry*, 2nd ed.; Longman Scientific & Technical: England, 1995; pp 152–153.

a simple relationship between enthalpy of reaction and pK_a of the acidic $\text{HEC}_6\text{H}_4\text{X}$ compounds can be established for both phenol and thiophenol systems. Both relationships display excellent linear fits ($R = 0.99$ for each).

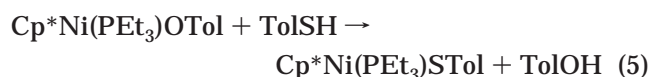
It has been suggested previously that oxidative addition reactions are principally driven by the acidity function of the incoming reagent, the feasibility of the oxidative addition depending on both this acidity function and the acid–base behavior/character of the metal center.¹⁵ The exothermicity of the oxidative addition at the electron-rich metal center can be modulated by as much as 10 kcal/mol by simply making subtle electronic variations.

This para-substituent effect is two-fold. The case of the electron-withdrawing NO_2 substituent is analyzed as a specific example. In the acid form, the electron-withdrawing character of the NO_2 fragment draws electron density from the H–E bond, weakening this bond compared to the unsubstituted parent acid (phenol or thiophenol). In the complex, the electron-withdrawing character of the substituents facilitate back-donation from the electron-rich metal center, leading to a stronger metal–heteroatom bond than in the unsubstituted parent. The measured enthalpy of reaction is therefore the most exothermic for the $-\text{NO}_2$ -substituted aryl-containing moieties since weaker bonds are broken and stronger bonds are formed.

Thermochemical Effects of Electronic Variations within the HEC_6H_5 Series (E = O (3), S (7), and Se (10)). The aryl substituent electronic effect is of significant importance. The thermochemical data allow us to examine the more obvious difference within a series of compounds which differ at the heteroatom, the effect on thermochemistry as a function of heteroatom–metal binding. The enthalpies of reaction within this series progress in the following order: phenol < thiophenol < selenophenol. The range spans 24 kcal/mol. The highest exothermicity measured within this series is for the selenophenol (-32.5 kcal/mol) and can be understood in terms of the acid–base concept. Arnett and Small have reported on the enthalpy of deprotonation of these compounds.¹⁶ The trend observed mimics the present one for enthalpies of oxidative addition. In Arnett's study, the enhanced acidity order selenyl > sulfhydryl > hydroxyl is also observed. This is explained in terms of the decreasing H–E bond strength as one goes down a group, which in turn may be related to the more diffuse bonding orbitals of larger atoms. The trend has also been quantified in the hard/soft concept of acids and bases¹⁷ and in the E and C bonding factorization of Drago.¹⁸ In a more quantitative fashion, Arnett has highlighted a relationship between enthal-

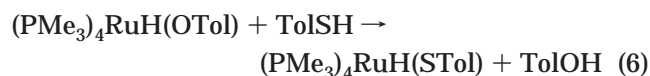
pies of deprotonation and pK_a values.^{19,20} Using these pK_a values, a relationship can be established between the acidity constants and the enthalpies of oxidative addition. The relationship displays a remarkable linear fit ($R = 0.95$) in view of pK_a solvent dependence.

We have recently performed a solution calorimetric study of a late-transition-metal system where similar chalcogenide moieties were bound to the metal center, eq 5.¹⁰ In the present system, a similar reaction



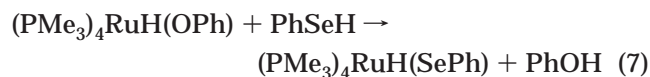
$$\Delta H_{\text{rxn}} = -14.0 \text{ kcal/mol}$$

enthalpy can be calculated from the thermochemical data, eq 6. The enthalpy difference between the two



$$\Delta H_{\text{calcd}} = -24.2 \text{ kcal/mol}$$

systems is 10 kcal/mol, favoring ruthenium. The nickel system includes a π ligand (Cp^*), therefore the overall π -bonding interaction with the incoming fragment may be decrease in view of this alternative pathway to channel π -electron density. In the present ruthenium system, this enthalpy difference between the alkoxide and sulfide is 24 kcal/mol. The ancillary ligation is comprised of excellent σ -donor ligands which do not possess π -acceptor properties. This ruthenium system is an excellent example of an electron-rich system that is unable to behave as a π acceptor but more than likely back-donates electron density into π orbitals of incoming ligand fragments. Therefore, the moiety most capable of accepting electron density from the metal center will have the largest enthalpy of oxidative addition. This is exactly what is observed since electron-withdrawing groups on the aryl substituent make the chalcogen-containing fragment more acidic, enabling electron density to be channeled back into the incoming π system. This preference for second-row main-group elements has been observed by Bryndza and Bercaw²¹ and Glueck²² for the $(\text{DPPE})\text{PtMeX}$ system. This trend appears slightly more accentuated for third-row main-group elements, eq 7.



$$\Delta H_{\text{calcd}} = -26.4 \text{ kcal/mol}$$

Structural Determination of $(\text{PMe}_3)_4\text{Ru}(\text{SC}_6\text{H}_5)\text{H}$ (7). To gain insight into the bonding patterns at play in this system, a structural determination of complex 7

(14) (a) For pK_a value of phenols, see: *The Chemistry of Functional Groups: the Chemistry of the Hydroxyl Group, part 1*; Patai, S., Ed.; Interscience Publishers: New York, 1971; pp 374–375. (b) For pK_a value of thiophenols, see: *The Chemistry of Functional Groups: the Chemistry of the Thiol Group, part 1*; Patai, S., Ed.; Interscience Publishers: New York, 1971; p 401.

(15) Vaska, L. *Acc. Chem. Res.* **1968**, *1*, 335–344.

(16) Arnett, E. M.; Small, L. E. *J. Am. Chem. Soc.* **1977**, *99*, 808–816.

(17) Pearson, R. G. In *Advances in Linear Free Energy Relationships*; Chapman, N. B., Shorter, J., Eds.; Plenum Press: New York, 1972.

(18) Drago, R. S. *Applications of Electrostatic-Covalent Models in Chemistry*; Surfside: Gainesville, FL, 1994.

(19) Arnett, E. M.; Moriarity, T. C.; Small, L. E.; Rudolph, R. P.; Quirk, R. P. *J. Am. Chem. Soc.* **1973**, *95*, 1492–1495.

(20) In the present case, the relationship is somewhat restrictive since no pK_a value has been reported for the selenol. A value can be determined (4.6 in water) by extrapolation of the relationship discussed in ref 19.

(21) Bryndza, H. E.; Fong, L. K.; Paciello, R. A.; Tam, W.; Bercaw, J. E. *J. Am. Chem. Soc.* **1987**, *109*, 1444–1456.

(22) Wicht, D. K.; Paisner, S. N.; Lew, B. M.; Glueck, D. S.; Yap, G. P. A.; Liable-Sands, L. M.; Rheingold, A. L.; Haar, C. M.; Nolan, S. P. *Organometallics* **1998**, *17*, 652–660.

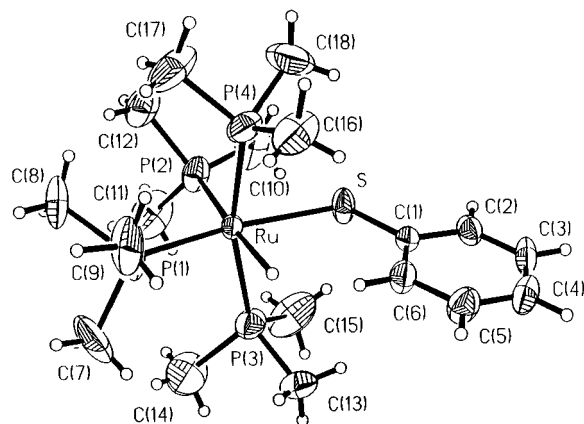


Figure 3. ORTEP of $(\text{PMe}_3)_4\text{Ru}(\text{SC}_6\text{H}_5)\text{H}$ (**7**). Ellipsoids are drawn in with 50% probability.

Table 2. Crystal Data and Details of the Structure Determination of $(\text{PMe}_3)_4\text{Ru}(\text{SC}_6\text{H}_5)\text{H}$ (**7**)

empirical formula	$\text{C}_{18}\text{H}_{42}\text{P}_4\text{RuS}$
fw	515.53
temp	295(2) K
wavelength	0.710 73 Å
cryst system	monoclinic
space group	$P2_1/c$
unit cell dimens	$a = 14.884(1)$ Å $b = 13.113(1)$ Å $c = 14.044(1)$ Å
	$\alpha = 90^\circ$ $\beta = 106.509(6)^\circ$ $\gamma = 90^\circ$
vol	$2628.0(3)$ Å ³
Z	4
density(calcd)	1.303 g/cm ³
abs coeff	9.20 cm^{-1}
$F(000)$	1080
cryst size	$0.32 \times 0.36 \times 0.48$ mm
range for data collection	$2.11\text{--}27.50^\circ$
index ranges	$-19 \leq h \leq 18, 17 \leq k \leq 0, 0 \leq l \leq 17$
no. of rflns collected	6191
no. of indep rflns	5946 ($R_{\text{int}} = 0.0180$)
refinement method	full-matrix least-squares on F^2
data/restraints/params	5306/12/265
goodness-of fit on F^2	1.033
final R indices [$I > 2\sigma(I)$]	$R1 = 0.0486, wR2 = 0.1037$
R indices (all data)	$R1 = 0.0858, wR2 = 0.1213$
ext coeff	0.00033(10)
largest diff peak and hole	1.047 and -0.704 e Å^{-3}

was undertaken. An ORTEP drawing of **7** is presented in Figure 3. The most striking feature of this pseudo-octahedral complex is the inequivalent Ru–P distances. The Ru–P(1) distance (2.2534 Å) is 0.09 Å shorter than the average Ru–P(2–4) distance (2.3402 Å). This bond shortening is a result of the trans influence²³ of the electron-withdrawing SPh group. This interaction is presumably resulting from the $d\pi\text{--}p\pi$ bonding mode. Of further significance are the Ru–S distance of 2.4579 Å, the Ru–H bond distance of 1.84 Å, and the S–Ru–H (81.2°), C(1)–S–Ru (117.2°), and P(1)–Ru–S (168.1°) bond angles. All other crystallographic and bond distance and angle data are presented in Tables 2 and 3. These data permit a comparison with the structural parameters previously reported for **2**.^{11b} On going from O to S, the Ru–E bond distance increases by 0.31 Å. The Ru–H distance increases by 0.1 Å. The average

Table 3. Selected Bond Distances (Å) and Bond Angles (deg) for $(\text{PMe}_3)_4\text{Ru}(\text{SC}_6\text{H}_5)\text{H}$ (**7**)

Bond Lengths			
Ru–P(1)	2.2534(12)	Ru–P(3)	2.3347(13)
Ru–P(4)	2.3374(13)	Ru–P(2)	2.3484(12)
Ru–S	2.4579(10)	Ru–H	1.84
S–C(1)	1.757(3)	P(1)–C(7)	1.773(8)
P(1)–C(8)	1.885(7)	P(1)–C(9)	1.910(7)
P(2)–C(10)	1.827(5)	P(2)–C(11)	1.823(6)
P(2)–C(12)	1.840(5)	P(3)–C(13)	1.805(5)
P(3)–C(14)	1.856(6)	P(3)–C(15)	1.819(5)
P(4)–C(16)	1.815(5)	P(4)–C(17)	1.832(5)
P(4)–C(18)	1.865(5)		
Bond Angles			
P(1)–Ru–P(3)	96.57(6)	P(1)–Ru–P(2)	99.71(4)
P(1)–Ru–P(4)	95.85(6)	P(1)–Ru–S	168.08(4)
P(1)–Ru–H	86.4	P(2)–Ru–P(3)	94.78(5)
P(2)–Ru–P(4)	93.56(5)	P(2)–Ru–S	92.20(4)
P(2)–Ru–H	173.6	P(3)–Ru–P(4)	163.65(4)
P(3)–Ru–S	82.97(4)	P(3)–Ru–H	82.5
P(4)–Ru–S	82.68(4)	P(4)–Ru–H	87.7
S–Ru–H	81.8	C(1)–S–Ru	117.27(10)
C(7)–P(1)–Ru	128.0(3)	C(8)–P(1)–Ru	120.0(3)
C(9)–P(1)–Ru	111.0(2)	C(11)–P(2)–Ru	120.0(2)
C(10)–P(2)–Ru	117.8(2)	C(13)–P(3)–Ru	115.3(2)
C(12)–P(2)–Ru	118.6(2)	C(14)–P(3)–Ru	122.5(2)
C(15)–P(3)–Ru	117.1(2)	C(17)–P(4)–Ru	124.9(2)
C(16)–P(4)–Ru	114.2(2)		
C(18)–P(4)–Ru	116.9(2)		

Ru–P bond lengths are longer in **7**. As in the case of **7**, the Ru–P bond trans to the main-group atom in **2** displays a trans influence, making it shorter than the other Ru–P length by 0.1 Å. The bond distance elongations observed in **7** (and discussed above) can be explained in terms of increased back-donation into the sulfur-containing moiety.

The structural differences between **2** and **7** are also apparent in the bond angles. The P(1)–Ru–E angle ($E = \text{O}$, 176.96° ; $E = \text{S}$, 168.08°) shows a more linear arrangement in **2**. The E–Ru–H angles ($E = \text{O}$, 101.15° ; $E = \text{S}$, 81.2°) show a closer distance between the aryl fragment and the hydride in **7**. The C(1)–E–Ru angles ($E = \text{O}$, 133.3° ; $E = \text{S}$, 117.2°) also display a more linear arrangement in **2**. These three pairs of angles reflect a significant bending of the aryl moiety toward the Ru–H fragment in **7**. This “bend” could be attributable to an effort to maximize the $d\pi\text{--}p\pi$ interaction and to minimize the electron lone-pair repulsions in the complex.

It would be desirable to extract bond energy data from the enthalpic information, yet as illustrated by the variation in metrical parameters between **2** and **7**, reorganization energy²⁴ renders such treatment impossible. The enthalpies of reaction encompass all energetic terms involved in the transformation (ethylene displacement, oxidative addition, and reorganization energy). The enthalpic terms are, however, a true gauge of the relative stability of these electron-rich complexes.

Conclusion

The rapid and quantitative nature of the reactivity of HEAr ($E = \text{O}, \text{S}, \text{Se}$) with **1** makes the determination of a relative stability scale possible for 10 ruthenium complexes. The enthalpy trend can be explained in terms of H–EAr acidity. The study of substituent

(23) Appleton, T. G.; Clark, H. C.; Manzer, L. E. *Coord. Chem. Rev.* **1973**, *10*, 335–422.

(24) Huang, J.; Haar, C. M.; Nolan, S. P.; Marshall, W. J.; Moloy, K. G. *J. Am. Chem. Soc.*, in press.

effects on HEAr allows for the construction of thermochemical relationships between enthalpies of reaction and substituent Hammett parameters. Single-crystal diffraction work on one complex $(\text{PMe}_3)_4\text{Ru}(\text{SC}_6\text{H}_5)\text{H}$ (**7**) permits comparisons between S^- - and O^- -containing complexes. In view of significant bond length and bond angle variations between the two complexes, we wish to stress that reorganization energy prohibits the direct translation of reaction enthalpies into bond strengths in the present system.

Experimental Section

General Consideration. All manipulations involving organoruthenium complexes were performed under argon using standard high-vacuum or Schlenk tube techniques or in a MBraun glovebox containing less than 1 ppm of oxygen and water. All phenols, thiophenols, and benzeneselenol were purchased from Aldrich and recrystallized or redistilled before use. Solvents were dried and distilled under argon before use employing standard drying agents.²⁵ Only materials of high purity, as indicated by NMR spectroscopy, were used in the calorimetric experiments. NMR spectra were recorded using a Varian Gemini 300 MHz spectrometer. Calorimetric measurements were performed using a Calvet calorimeter (Setaram C-80), which was periodically calibrated using the TRIS reaction²⁶ or the enthalpy of solution of KCl in water.²⁷ The experimental enthalpies for these two standard reactions compared very closely to literature values. This calorimeter has been previously described,²⁸ and typical procedures are described below. Experimental enthalpy data are reported with 95% confidence limits.

NMR Titrations. Prior to every set of calorimetric experiments involving a new HEAr, an accurately weighed amount (± 0.1 mg) of the organoruthenium complex was placed in a Wilmad screw-capped NMR tube fitted with a septum and C_6D_6 was subsequently added. The solution was titrated with a solution of the HEAr of interest by injecting the latter in aliquots through the septum with a microsyringe, followed by vigorous shaking. The reactions were monitored by ^{31}P and ^1H NMR spectroscopy, and the reactions were found to be rapid, clean, and quantitative. These conditions are necessary for accurate and meaningful calorimetric results and were satisfied for all organometallic reactions investigated.

Solution Calorimetry. Calorimetric Measurement of Reaction Between $(\text{PMe}_3)_4\text{Ru}(\text{C}_2\text{H}_4)$ (1**) and $p\text{-CH}_3\text{C}_6\text{H}_4\text{OH}$.** The mixing vessels of the Setaram C-80 were cleaned, dried in an oven maintained at 120°C , and then taken into the glovebox. A 20 mg sample of $(\text{PMe}_3)_4\text{Ru}(\text{C}_2\text{H}_4)$ was accurately weighed into the lower vessel, which was closed and sealed with 1.5 mL of mercury. Four milliliters of a stock solution of $p\text{-CH}_3\text{C}_6\text{H}_4\text{OH}$ (30 mg of $p\text{-CH}_3\text{C}_6\text{H}_4\text{OH}$ in 20 mL of C_6H_6) was added, and the remainder of the cell was assembled, removed from the glovebox, and inserted in the calorimeter. The reference vessel was loaded in an identical fashion with the exception that no organoruthenium complex was added to the lower vessel. After the calorimeter had reached thermal equilibrium at 30.0°C (about 2 h), the calorimeter was inverted, thereby allowing the reactants to mix. After the reaction had reached completion and the calorimeter had once again reached thermal equilibrium (ca. 2 h), the vessels were removed from the calorimeter. Conversion to $(\text{PMe}_3)_4\text{Ru}(\text{H})$ -

$(\text{OC}_6\text{H}_4\text{-}p\text{-CH}_3)$ was found to be quantitative under these reaction conditions. Control reactions with Hg and HEAr show no reaction. The enthalpy of reaction, -0.5 ± 0.2 kcal/mol, represents the average of five individual calorimetric determinations. The final enthalpy value listed in Table 1 (-4.1 ± 0.2 kcal/mol) represents the enthalpy of reaction with all species in solution. The enthalpy of solution of **1** (3.6 ± 0.1 kcal/mol) has therefore been subtracted from the -0.5 kcal/mol value. This methodology represents a typical procedure involving all organometallic compounds and all reactions investigated in the present study.

Enthalpy of Solution of $(\text{PMe}_3)_4\text{Ru}(\text{C}_2\text{H}_4)$ (1**).** To consider all species in solution, the enthalpy of solution of $(\text{PMe}_3)_4\text{Ru}(\text{C}_2\text{H}_4)$ (**1**) had to be directly measured. This was performed by using a similar procedure as the one described above, with the exception that no HEAr was added to the reaction cell. The enthalpy of solution, 3.6 ± 0.1 kcal/mol, represents the average of five individual determinations.

Synthesis. The compound $(\text{PMe}_3)_4\text{Ru}(\text{C}_2\text{H}_4)$ (**1**) was synthesized according to literature procedures.^{11b} Other organoruthenium complexes, $(\text{PMe}_3)_4\text{Ru}(\text{H})(\text{OC}_6\text{H}_4\text{-}p\text{-CH}_3)$ (**2**), $(\text{PMe}_3)_4\text{Ru}(\text{H})(\text{OC}_6\text{H}_5)$ (**3**), $(\text{PMe}_3)_4\text{Ru}(\text{H})(\text{OC}_6\text{H}_4\text{-}p\text{-Cl})$ (**4**), $(\text{PMe}_3)_4\text{Ru}(\text{H})(\text{OC}_6\text{H}_4\text{-}p\text{-NO}_2)$ (**5**), and $(\text{PMe}_3)_4\text{Ru}(\text{H})(\text{SC}_6\text{H}_4\text{-}p\text{-CH}_3)$ (**6**) have been previously reported. Experimental synthetic procedures, leading to the isolation of previously unreported complexes, are described below.

$(\text{PMe}_3)_4\text{Ru}(\text{H})(\text{SC}_6\text{H}_5)$ (7**).** In the glovebox, 60.6 mg (0.140 mmol) of $(\text{PMe}_3)_4\text{Ru}(\text{C}_2\text{H}_4)$ and 10 mL of pentane were charged into a 50 mL flask. To this solution, 15.4 mg (0.140 mmol) of HSC_6H_5 was added. The reaction mixture was stirred for 3 h, during which time a precipitate formed. The solution was filtered and evacuated to dryness. The resulting yellow powder was recrystallized from pentane/methylene chloride to yield amber crystals, which were dried thoroughly under vacuum. Yield: 41 mg (57%). ^1H NMR (C_6D_6 , mult, $J = \text{Hz}$): δ (ppm) 8.33 (d, $J = 8.1$, 2 H, Ph), 7.21 (m, 2 H, Ph), 6.92 (t, $J = 7.8$, 1 H, Ph), 1.28 (t, $J = 3.0$, 18 H, PMe_3), 1.12 (d, $J = 5.4$, 9 H, PMe_3), 1.08 (d, $J = 9.6$, 9 H, PMe_3), -8.67 (dt, $J = 28.2$, $J = 87.6$, 1 H, Ru-H). $^{31}\text{P}\{^1\text{H}\}$ NMR (C_6D_6): δ (ppm) 2.56 (m, $J = 24.4$, $J = 29.8$), -7.55 (m, $J = 26.0$), -17.91 (m). Anal. Calcd for $\text{C}_{18}\text{H}_{42}\text{P}_4\text{SRu}$: C, 41.93; H, 8.21. Found: C, 41.90; H, 7.97.

$(\text{PMe}_3)_4\text{Ru}(\text{H})(\text{SC}_6\text{H}_4\text{-}p\text{-Cl})$ (8**).** In a manner analogous to **7**, **8** was isolated as amber crystals in 54% yield. ^1H NMR (C_6D_6 , mult, $J = \text{Hz}$): δ (ppm) 8.13 (d, $J = 8.4$, 2 H, Ph), 7.13 (d, $J = 9.0$, 2 H, Ph), 1.23 (t, $J = 2.7$, 18 H, PMe_3), 1.08 (d, $J = 4.8$, 9 H, PMe_3), 1.05 (d, $J = 6.9$, 9 H, PMe_3), -8.82 (dt, $J = 33.1$, $J = 81.0$, 1 H, Ru-H). $^{31}\text{P}\{^1\text{H}\}$ NMR (C_6D_6): δ (ppm) 2.00 (m, $J = 19.1$, $J = 24.3$), -8.17 (m, $J = 25.3$), -18.41 (m). Anal. Calcd for $\text{C}_{18}\text{H}_{41}\text{ClP}_4\text{SRu}$: C, 39.31; H, 7.51. Found: C, 39.60; H, 7.38.

$(\text{PMe}_3)_4\text{Ru}(\text{H})(\text{SC}_6\text{H}_4\text{-}p\text{-NO}_2)$ (9**).** In a manner analogous to **7**, **9** was isolated as purple microcrystals in 86% yield. ^1H NMR (C_6D_6 , mult, $J = \text{Hz}$): δ (ppm) 8.31 (m, 2 H, Ph), 7.41 (m, 2 H, Ph), 1.33 (t, $J = 3.0$, 18 H, PMe_3), 1.25 (d, $J = 4.5$, 9 H, PMe_3), 1.22 (d, $J = 7.5$, 9 H, PMe_3), -8.82 (dt, $J = 27.3$, $J = 87.0$, 1 H, Ru-H). $^{31}\text{P}\{^1\text{H}\}$ NMR (C_6D_6): δ (ppm) 2.64 (m, $J = 31.6$, $J = 19.4$), -7.79 (m, $J = 40.1$), -18.88 (m). Anal. Calcd for $\text{C}_{18}\text{H}_{41}\text{NO}_2\text{P}_4\text{SRu}$: C, 38.57; H, 7.37; N, 2.50. Found: C, 38.54; H, 7.25; N, 2.73.

$(\text{PMe}_3)_4\text{Ru}(\text{H})(\text{SeC}_6\text{H}_5)$ (10**).** In a manner analogous to **7**, **10** was isolated as amber crystals in 56% yield. ^1H NMR (C_6D_6 , mult, $J = \text{Hz}$): δ (ppm) 8.48 (d, $J = 7.8$, 2 H, Ph), 7.10 (m, $J = 6.3$, 2 H, Ph), 6.98 (t, $J = 6.0$, 1 H, Ph), 1.28 (t, $J = 3.0$, 18 H, PMe_3), 1.04 (d, $J = 5.4$, 9 H, PMe_3), 1.01 (d, $J = 9.6$, 9 H, PMe_3), -9.05 (dt, $J = 25.8$, $J = 85.5$, 1 H, Ru-H). $^{31}\text{P}\{^1\text{H}\}$ NMR (C_6D_6): δ (ppm) 2.59 (m, $J = 30.5$), -10.40 (m,

(25) Perrin, D. D.; Armarego, W. L. F. *Purification of Laboratory Chemicals*, 3rd ed.; Pergamon Press: New York, 1988.

(26) Ojelund, G.; Wadsö, I. *Acta Chem. Scand.* **1968**, *22*, 1691–1699.

(27) Kilday, M. V. *J. Res. Natl. Bur. Stand. U.S.* **1980**, *85*, 467–481.

(28) (a) Nolan, S. P.; Hoff, C. D.; Landrum, J. T. *J. Organomet. Chem.* **1985**, *282*, 357–362. (b) Nolan, S. P.; Lopez de la Vega, R.; Hoff, C. D. *Inorg. Chem.* **1986**, *25*, 4446–4448.

(29) This complex was first synthesized using $(\text{PMe}_3)_4\text{RuH}_2$ and the appropriate phenol, see: Osakada, K.; Ohshiro, K.; Yamamoto, A. *Organometallics* **1991**, *10*, 404–410.

$J = 28.9$), -17.77 (m). Anal. Calcd for $\text{C}_{18}\text{H}_{42}\text{P}_4\text{SeRu}$: C, 38.44; H, 7.53. Found: C, 38.61; H, 7.94.

Structure Determination of $(\text{PMe}_3)_4\text{Ru}(\text{H})(\text{SC}_6\text{H}_5)$ (7**).** Crystals of $(\text{PMe}_3)_4\text{Ru}(\text{H})(\text{SC}_6\text{H}_5)$ suitable for X-ray crystallography were grown in pentane. A crystal of $(\text{PMe}_3)_4\text{Ru}(\text{H})(\text{SC}_6\text{H}_5)$ was sealed in a capillary tube and then optically aligned on the goniostat of a Siemens P4 automated X-ray diffractometer. The reflections that were used for the unit cell determination were located and indexed by the automatic peak search routine XSCANS.³⁰ The corresponding lattice parameters and orientation matrix were provided from a nonlinear least-squares fit of the orientation angles of 54 centered reflections ($10^\circ < 2\theta < 25^\circ$) at 22°C . The refined lattice parameters and other pertinent crystallographic information are summarized in Table 2.

Intensity data were measured with graphite-monochromated Mo $K\alpha$ radiation ($\lambda = 0.71073 \text{ \AA}$) and variable ω scans ($4.0\text{--}20.0^\circ/\text{min}$). Background counts were measured at the beginning and at the end of each scan with the crystal and counter kept stationary. The intensities of three standard reflections were measured after every 100 reflections. Their combined intensity decreased by 2% during data collections. The data were corrected for Lorentz–polarization and the symmetry-equivalent reflections were averaged. An empirical absorption correction (range of transmission coefficients: $0.736\text{--}0.775$) based upon the ψ scans measured for 8 reflections ($\chi \approx 90^\circ$, $2\theta = 6\text{--}36^\circ$) was applied.

The initial coordinates for the non-hydrogen atoms were determined with a combination of direct methods and difference Fourier calculations performed with algorithms provided by SHELXTL IRIS operating on a Silicon Graphics IRIS Indigo workstation. During the course of the structural refinement, it became evident that the three carbons of the trimethylphosphine ligand trans to the thiolate ligand were disordered. The

positions of C(7), C(8), and C(9) were refined using a two-site model with the P–C and C–C distances restrained to 1.820 ± 02 and $2.800 \pm 02 \text{ \AA}$, respectively. The refined occupancy factor indicated that two disordered sites were present in a 60:40 ratio. The position of the hydride ligand was located and refined isotropically. Full-matrix least-squares refinement, based upon the minimization of $\sum w_i |F_o^2 - F_c^2|^2$, with $w_i^{-1} = \sigma^2(F_o^2) + (0.0430P)^2 + 2.7585P$, where $P = (\text{Max}(F_o^2, 0) + 2F_c^2)/3$, was performed with SHELXL-93.³¹ After convergence, the final discrepancy indices were $R1 = 0.0486$ and $wR2 = 0.1037$ for 4037 reflections with $I > 2\sigma(I)$ and the overall GOF value was 1.033. Selected interatomic distances and angles are listed in Table 3. An ORTEP view of the complex is presented in Figure 3.

Acknowledgment. S.P.N. acknowledges the National Science Foundation (Grant No. CHE-9631611) and Dupont (Educational Aid Grant) for financial support of this research. J.L.P acknowledges the financial support provided by the Chemical Instrumentation Program of the National Science Foundation (Grant No. CHE-9120098) for the acquisition of a Siemens P4 X-ray diffractometer by the Department of Chemistry at West Virginia University.

Supporting Information Available: Tables of anisotropic thermal parameters, positional parameters, bond angles, and bond distances for **7** (7 pages). Ordering and Internet access information are given on any current masthead page.

OM980253P

(30) XSCANS (version 2.0) is a diffractometer control system developed by Siemens Analytical X-ray Instruments, Madison, WI.

(31) SHELXL-93 is a FORTRAN-77 program (Prof. G. Sheldrick, Institut für Anorganische Chemie, University of Göttingen, D-37077, Göttingen, Germany) for single-crystal X-ray structural analysis.